J. Human Ergol., **29**: 35-52, 2000

INNERVATION ZONES OF THE UPPER AND LOWER LIMB MUSCLES ESTIMATED BY USING MULTICHANNEL SURFACE EMG

KENJI SAITOU[1*], TADASHI MASUDA[2], DAISAKU MICHIKAMI[3], RYUHEI KOJIMA[4], AND MORIHIKO OKADA[5]

[1] *Institute of Health and Sport Sciences, University of Tsukuba, 1-1-1 Tennoudai, Tsukuba 305-8574, Japan*
[2] *National Institute of Bioscience and Human Technology, Human Environment System Department, 1-1 Higashi, Tsukuba 305-8566, Japan*
[3] *Research Institute of Environmental Medicine, Nagoya University, 1 Furo-cho, Chigusa-ku, Nagoya 464-8601, Japan*
[4] *Department of Physical Therapy, Saitama Medical School Junior College, 38 Morohongo, Moroyama-cho, Iruma-gun, Saitama-ken 350-0495, Japan*
[5] *Center for Tsukuba Advanced Research Alliance, University of Tsukuba, 1-1-1 Tennoudai, Tsukuba 305-8577, Japan*
[*Present] *Department of Civil Engineering, Faculty of Science and Engineering, Saga University, 1 Honjo, Saga 840-8502, Japan*

The distribution of innervation zones was investigated in 3 subjects for 17 muscles and 8 muscle groups in the upper and lower limb, by detecting bi-directional propagation of motor unit action potentials (MUAPs) with the multichannel surface electrode array. Clarification of the distribution of innervation zones depended on the ease in detecting the propagation of MUAPs and the actual scattering of innervation zones, which were closely related with muscle morphology with respect to the arrangements of muscle fibers. In muscles having fibers running parallel to each other, such as the biceps brachii, intrinsic hand muscles, vastus lateralis and medialis, tensor fasciae latae, peronei, soleus, tibialis anterior, and hypothenar muscles in the foot, it was relatively easy to detect the propagating MUAPs, and the innervation zones were distributed in a relatively narrow band around muscle belly. On the other hand, in muscles with a complicated structure including pinnation of muscle fibers, in-series muscle fibers and aponeurotic tissues, such as the deltoid, flexors and extensors in the forearm, rectus femoris, sartorius, hamstrings and gastrocnemius, it was more difficult to detect the propagating MUAPs and to identify the innervation zones, which were widely scattered or distributed in complex configurations.
The distribution of the innervation zones clarified in the present study can be used to find the optimal location of electrodes in surface EMG recordings and of stimulus electrodes in the functional and therapeutic electrical stimulations. It may also be useful in motor point biopsy for diagnosis of neuromuscular diseases as well as in the botulinum toxin injection for the treatment of spasticity.

INTRODUCTION

Surface EMG is increasingly popularized in such research field as ergology, sports sciences and rehabilitation, as a tool to monitor the electrical activity and metabolic conditions including local fatigue of muscles. It has been well documented that the surface EMGs are affected by the electrode conditions and the characteristics of subcutaneous tissues (Zipp, 1978; De Luca, 1984; Roy et al., 1986). In recent years, it has been clarified that the surface EMGs are also affected by the position of recording electrodes with respect to the innervation zones and tendons (Basmajian and De Luca, 1985; Roy et al., 1986; Saitou et al., 1996; Rainoldi et al., 2000). We designate macroscopically the assembly of motor endplates as an innervation zone.

If the electrodes are placed on the innervation zones, the surface EMG waveforms are compli-

Received for publication May 22, 2000

cated by mutual interferences of motor unit action potentials (MUAPs) (Basmajian and De Luca, 1985; Saitou et al., 1991), leading to an incorrect estimation of the power spectra and muscle fiber conduction velocity (MFCV). Some MUAPs may be cancelled out in the case of bipolar lead (Basmajian and De Luca, 1985), which yields a reduced EMG magnitude. Thus, the monitoring of muscular activity and detection of muscle fatigue could be affected by the electrode placements. These situations warrant advising the placing of electrodes between the innervation zones and tendons (Basmajian and De Luca, 1985; Roy et al., 1986; Saitou et al., 1996).

MUAPs arise from the innervation zones and propagate bidirectionally along the muscle fibers to both fiber ends. It is therefore possible to find innervation zones by detecting the bidirectional propagation of MUAPs (Arendt-Nielsen and Zwarts, 1989; Masuda et al., 1983). By using this method, Masuda and Sadoyama (1987) reported that the innervation zones could be identified in 19 out of 26 muscles studied. However, they did not report the actual distribution of innervation zones in each muscle. Subsequently, Masuda and Sadoyama (1991) showed the detailed distribution of the innervation zones in the biceps brachii muscle, and Shiraishi et al. (1995) clarified the innervation zones in the trapezius and the lattissimus dorsi muscles. For other muscles than the above, the distribution of innervation zones has not been reported yet.

As mentioned above, however, knowledge of the distribution of the innervation zones in the muscles concerned is important for correctly estimating the surface EMG parameters required. Thus we attempted in this paper to clarify the distribution of innervation zones in the upper and the lower limb muscles, for most of which the distribution has not been reported.

METHODS

Subjects and Procedures

The subjects were 6 normal healthy males aged from 22 to 24. Three of them participated in the measurements of the upper and lower limb muscles, respectively. Six muscles (deltoid, biceps brachii, triceps brachii, brachioradialis, flexor carpi ulnaris, and first dorsal interosseous) and 5 muscle groups (flexors in the forearm, extensors in the forearm, extensors of the pollex, thenar muscles, and hypothenar muscles) in the upper limb, and 11 muscles (rectus femoris, vastus lateralis, vastus medialis, sartorius, tensor fasciae latae, semitendinosus, long head of the biceps femoris, tibialis anterior, soleus, gastrocnemius, and abductor hallucis) and 3 muscle groups (peronei, extensors in the foot, and hypothenar muscles) in the lower limb were examined. In all the cases the right hand side was measured.

The manners to elicit volitional contractions in the muscles or muscle groups examined are summarized in Tables 1 and 2. External load for the subjects to resist was produced manually by the experimenter. In each measurement, the subjects exerted the nearly maximal force isometrically for about 3 sec. The muscles were contracted individually except the 9 muscle groups, which were co-contracted synchronously. To avoid muscular fatigue, the subjects took at least a 2-min rest between the contractions.

EMG Signal Acquisition and Processing

Surface EMG signals were picked up with an electrode array consisting of 17 stainless steel wire contacts (Figure 1). Each contact was 0.75 mm thick and 5 mm long. The contacts were arranged parallel to each other at an interval of 2.5 mm. The electrode array was placed along the muscle fiber direction. To clarify the innervation zones over the whole surface of each muscle, the electrode array was moved from location to location at intervals of about 5 mm. For each muscle, EMG signals were recorded 30 to 90 times. Experimental time was at most about 3 hours in the deltoid.

Sixteen EMG signals were derived bipolarly from the pairs of adjacent contacts in the electrode array. The ground electrode was placed on the sternum. The derived signals were filtered with a

Table 1. Muscles and muscle groups investigated in the upper limb, selective test movements, and testing position of the limb.

Muscle(s) examined	Selective test movements	Testing position of the limb
Deltoid	Abduction, flexion, and extension of the shoulder for the intermediate, anterior, and posterior part, respectively	Upper limb suspended by subject's body, with the elbow extended
Biceps brachii	Flexion of the elbow	The same as above except that the elbow is somewhat flexed
Triceps brachii	Extension of the elbow	The same as above
Brachioradialis	Flexion of the elbow and radial flexion of the wrist	Shoulder and elbow joints somewhat flexed, with the forearm in the neutral position
Flexor carpi ulnaris	Ulnar flexion of the wrist	The same as above except that the forearm is supinated
Flexors in the forearm	Flexion of the wrist	The same as above
Extensors in the forearm	Extension of the wrist	The same as above except that the forearm is pronated
Extensors of the pollex	Abduction of the thumb	The same as above
Thenar muscles	Flexion of the thumb	The same as above except that the forearm is supinated
Hypothenar muscles	Abduction of the little finger	The same as above
First dorsal interosseous	Abduction of the index finger	The same as above except that the forearm is pronated

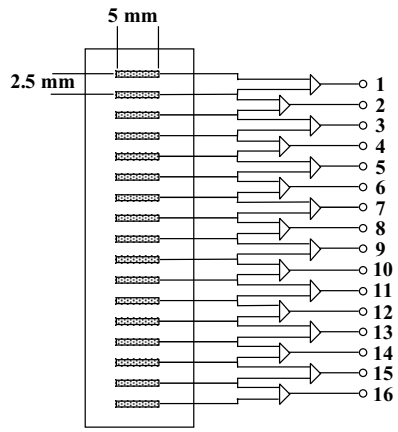

Fig. 1. A sixteen-channel surface electrode array consisting of 17 stainless steel wire contacts.

Table 2. Muscles and muscle groups investigated in the lower limb, selective test movements, and testing position of the limb.

Muscle(s) examined	Selective test movements	Testing position of the limb
Rectus femoris, vastus lateralis, and vastus medialis	Extension of the knee	Knee joint flexed at right angles while the subject seated
Sartorius	Flexion of the hip and extension of the knee	The same as above
Tensor fasciae latae	Abduction of the hip	Hip and knee extended while the subject lying on one's side
Semitendinosus and biceps femoris	Flexion of the knee	Knee joint somewhat flexed while the subject lying prone
Tibialis anterior	Dorsi-flexion of the ankle	Knee joint flexed at right angles while the subject seated
Peronei	Eversion of the foot	The same as above
Soleus and gastrocnemius	Plantal-flexion of the ankle	Standing upright
Extensors in the foot	Extension of the toes	The same as above
Abductor hallucis	Flexion and abduction of the hallux	Ankle joint in neutral position and knee joint extended, while the subject sitting down
Hypothenar muscles	Flexion and abduction of the fifth toe	The same as above

power-line frequency notch filter and amplified in gain of 60 dB over the frequency range of 53-1000 Hz (Polygraph 360, NEC San-ei, Tokyo, Japan). The signals were then digitized with a sampling frequency of 5 kHz and a resolution of 12 bits. The sampled length was 4096 points, equivalent to about 0.8 sec duration.

The sampled EMG signals were displayed on a CRT of a personal computer, and the source of the propagation was determined by visual analysis. If the EMG signals are picked up from the skin just over the innervation zones, MUAPs propagating in the opposite direction cancel each other out, and consequently the EMG shows low amplitude. Around the innervation zones, MUAPs propagating in the opposite directions yield EMG waveforms symmetrical with respect to the source of the propagation and with a constant time-delay between each channel (Figure 2). From these propagation patterns, we can identify the position of innervation zones (Masuda and Sadoyama, 1991).

RESULTS

Bidirectional propagations of MUAPs were detected by a ratio from 20 to 100% in the muscles studied. The detection was easiest in the biceps brachii, whereas it was most difficult in the intermediate part of the deltoid, rectus femoris, long head of biceps femoris, and semitendinosus. In the vastus lateralis, vastus medialis, tibialis anterior and extensors in the foot, the detection was easier. Because the forearm muscles were generally thin and small, it was difficult to identify individual muscles. Therefore these muscles, excluding the brachioradialis and the flexor carpi ulnaris, were

summarized as flexors in the forearm and extensors in the forearm.

Deltoid

In the deltoid, bidirectional propagation was easily observed in the anterior and the posterior parts. In the intermediate part, however, complex waveforms were frequently observed. In this area some MUAPs did not show a clear source of propagation as shown in Figure 2, whereas some showed one-directional propagation, and others showed a symmetrical configuration with respect to the source but without propagation (Figure 3). These waveforms made the identification of innervation zones

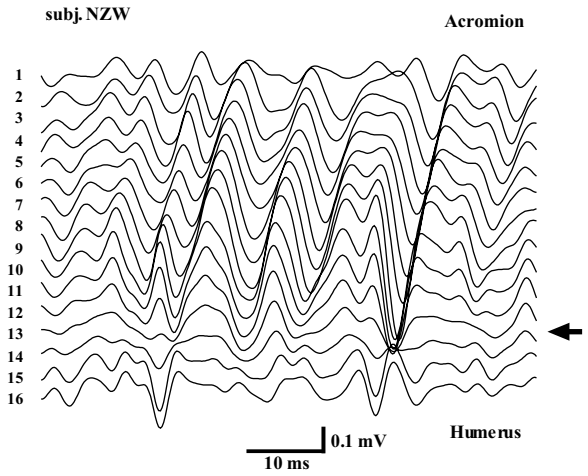

Fig. 2. Waveforms of the surface EMGs detected from the intermediate part of the deltoid. The potentials propagate bidirectionally from the source near the 13th channel as indicated by an arrow. Accordingly, the innervation zone is estimated to be located at the position of 13th channel.

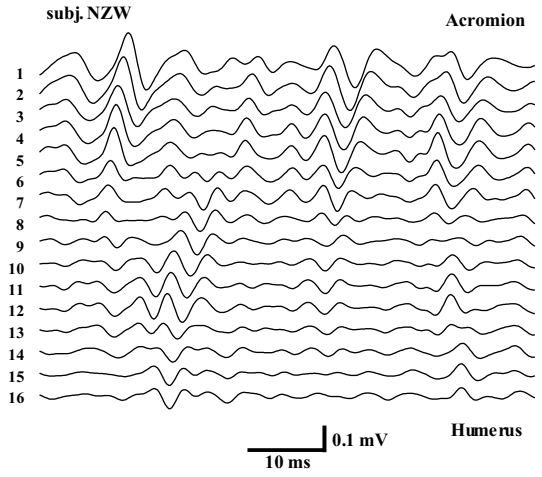

Fig. 3. Waveforms of the surface EMGs detected from the intermediate part of the deltoid. These waveforms exemplify propagation without source, one-directional propagation, and no propagation. The innervation zones cannot be identified from these waveforms.

impossible. The innervation zones were found to be scattered in a wide area, or distributed in an inverse S-shaped configuration from the clavicle to the spine of the scapula (Figure 4).

Biceps brachii

The biceps brachii showed a clear propagation of MUAPs. The innervation zones were distributed in a narrow band around the muscle belly. In subject OKM, the innervation zones in the short head were scattered in a wider band (Figure 5a).

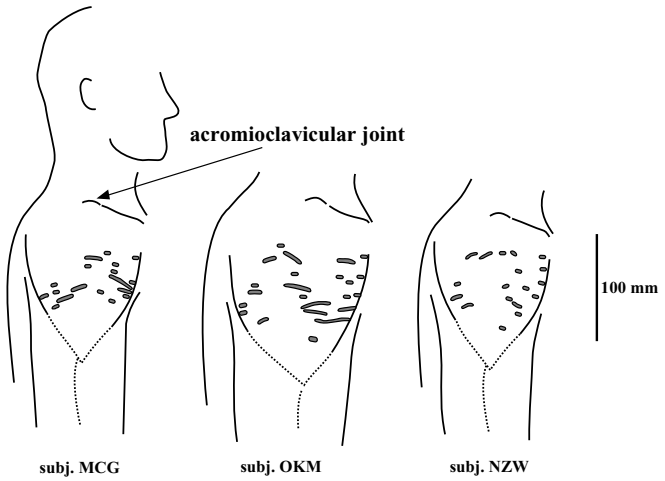

Fig. 4. Distribution of the innervation zones in the deltoid.

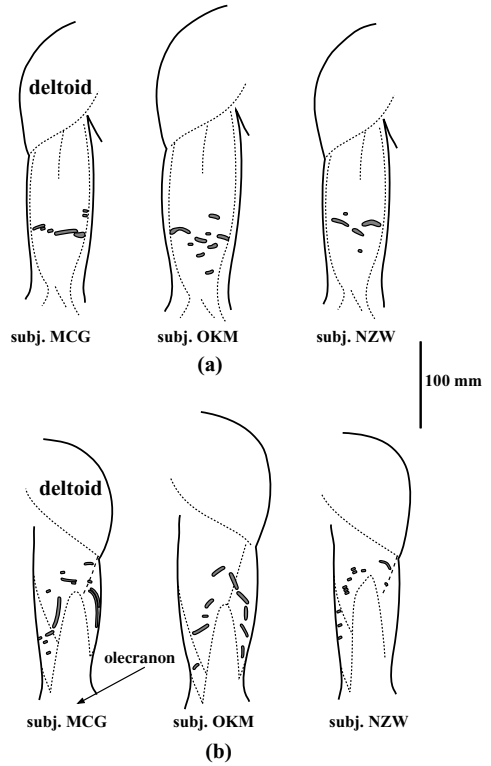

Fig. 5. Distribution of the innervation zones in the biceps brachii (a) and the triceps brachii (b).

Triceps brachii

The triceps brachii showed clear propagation of MUAPs in the long head and in the lateral head except in subject NZW (Figure 6). In the medial head, however, the propagation was unclear and definition of innervation zones was uncertain. The innervation zones were distributed in an inverse U-shaped area around the tendon of the triceps brachii (Figure 5b).

Forearm muscles

In the flexors in the forearm, clear propagation was detected in the proximal area. The innervation zones of the pronator teres, flexor carpi radialis and palmaris longus were scattered in an area spanning from the middle length of the forearm to the elbow (Figure 7a). The innervation zones of the flexor carpi ulnaris were also scattered around the muscle belly (Figure 7b). In the brachioradialis, clear propagation of MUAPs was not detected in an area proximal to the elbow. The innervation zones in this muscle were distributed in a wide area ranging from the middle length of the forearm to the elbow (Figure 7c). In the distal area of the forearm in subjects OKM and NZW, a small number of innervation zones were identified presumably in the flexor digitorum superficialis.

In the extensors in the forearm, the propagation of MUAPs was observed over longer distances. The extensors of the pollex showed clear propagation. The innervation zones in the extensors in the forearm (extensor carpi radialis, extensor digitorum, and extensor carpi ulnaris) were scattered in a wide area. In the proximal area of subject NZW, no innervation zone could be identified (Figure 7d).

Hand muscles

Clear propagation of MUAPs was detected easily from the thenar and hypothenar muscles as well as from the first dorsal interosseous (Figure 8). The innervation zones of the thenar and hypothenar muscles were distributed in an area about 20 mm wide (Figure 9a). In the first dorsal interosseous the innervation zones were distributed in a narrow band around the muscle belly (Figure 9b).

Rectus femoris, vastus lateralis, and vastus medialis

The vastus lateralis and medialis showed clear propagation of MUAPs. The innervation zones were distributed in the middle of muscle fibers running upward from the common tendon of the quadriceps femoris (Figure 10a). Clear propagation of MUAPs as shown in Figure 11 have been

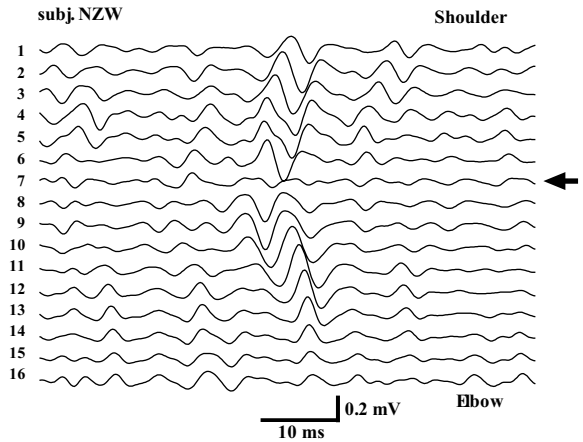

Fig. 6. Waveforms of the surface EMGs detected from the long head of the triceps brachii. Arrow indicates the estimated position of the source of the MUAP propagation.

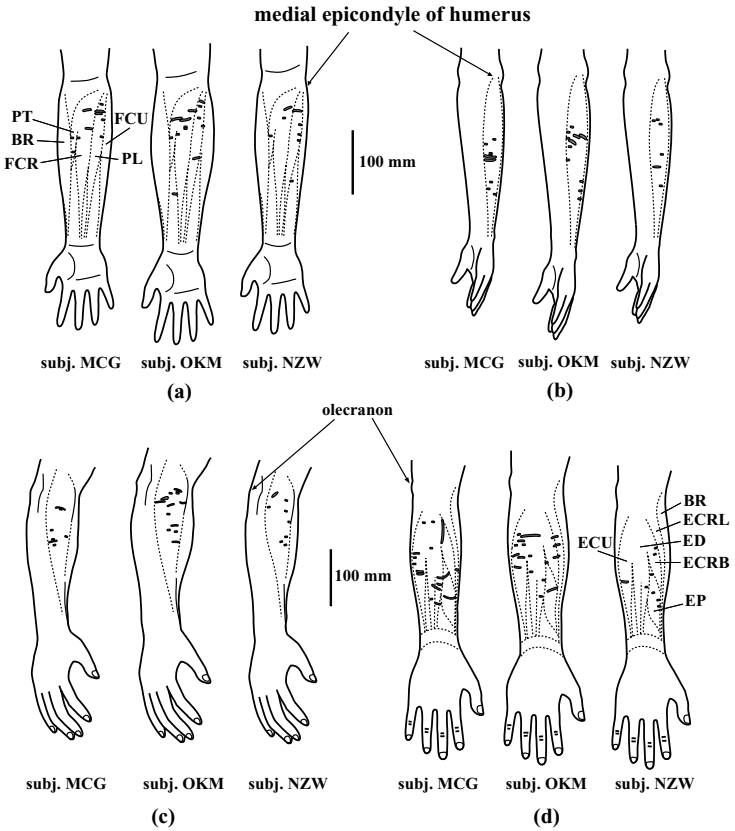

Fig. 7. Distribution of the innervation zones in the flexors in the forearm (a), the flexor carpi ulnaris (b), the brachioradialis (c), and the extensors in the forearm (d). PT, BR, FCR, PL, and FCU in (a) indicate pronator teres, brchioradialis, flexor carpi radialis, palmalis longus, and flexor carpi ulnaris, respectively. ECU, ECRL, ED, ECRB, and EP in (d) indicate extensor carpi ulnaris, extensor carpi radialis longus, extensor digitorum, extensor carpi radialis brevis, and extensors of pollex, respectively.

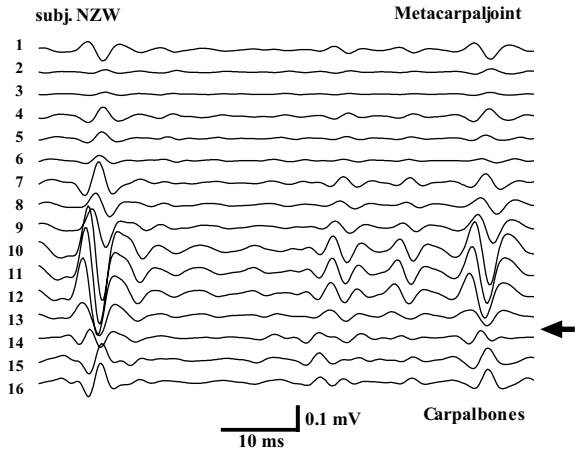

Fig. 8. Waveforms of the surface EMGs detected from the first dorsal interosseous. Arrow indicates the estimated position of the source of the MUAP propagation.

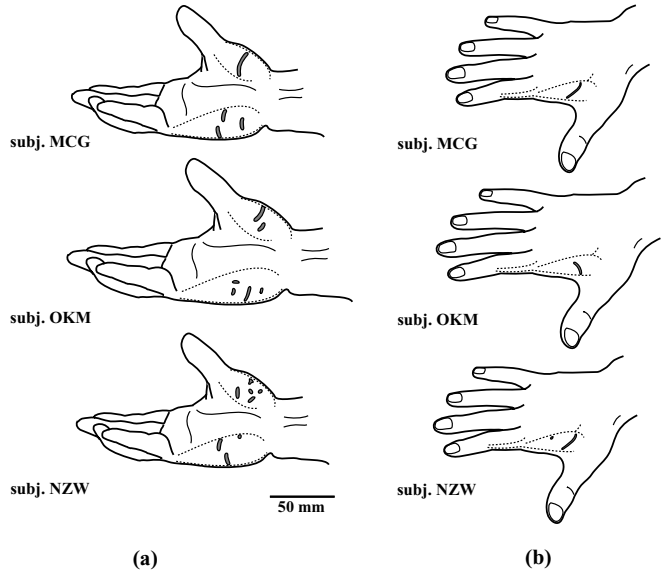

Fig. 9. Distribution of the innervation zones in the thenar and hypothenar muscles (a) and in the first dorsal interosseous (b).

rarely seen in the rectus femoris. The innervation zones of this muscle were distributed around the muscle belly irregularly (Figure 10a). In subject NSY, the innervation zones were not identified in the rectus femoris.

Sartorius

Clear propagation of MUAPs was detected easily from the part near the anterior superior iliac spine (Figure 12), whereas not clearly detected from the median and distal part of muscle belly. The innervation zones were scattered in the whole area of the muscle belly (Figure 10b).

Tensor fasciae latae

Clear propagation of MUAPs was detected from the muscle belly. The innervation zones were distributed in the median part and in the distal part near the vastus lateralis (Figure 13a).

Semitendinosus and long head of biceps femoris

It was difficult to detect the propagation of MUAPs from the distal part of the hamstrings by positioning the surface electrode array, probably due to the influence of tendinous tissues, intermediate tendon and muscle structure that is pinnate or bipinnate in configuration. Clear propagation of MUAPs could be detected more easily from the proximal part (Figure 14). Therefore, more innervation zones were identified in the proximal part than in the distal part (Figure 13b).

Tibialis anterior

In the tibialis anterior, clear propagation patterns were detected in the middle one third of the lower leg length. The innervation zones were detected in a narrow band around the muscle belly in subject HBY (Figure 15a). On the contrary, the innervation zones of subject NKI and NSY were scattered over the muscle belly in which the propagation patterns were detected.

Peronei

The propagation of MUAPs was detected from the muscle belly in the proximal half of the

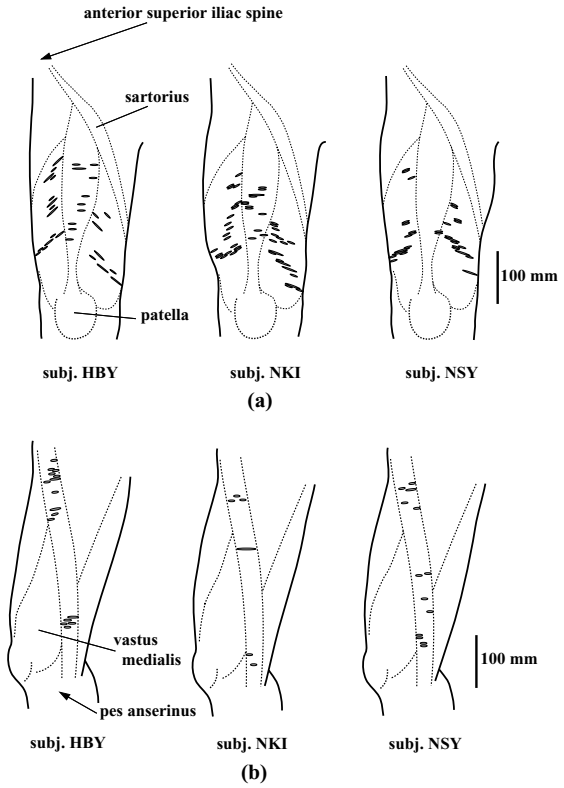

Fig. 10. Distribution of the innervation zones in the vastus lateralis, the rectus femoris and the vastus medialis (a) and in the sartorius (b).

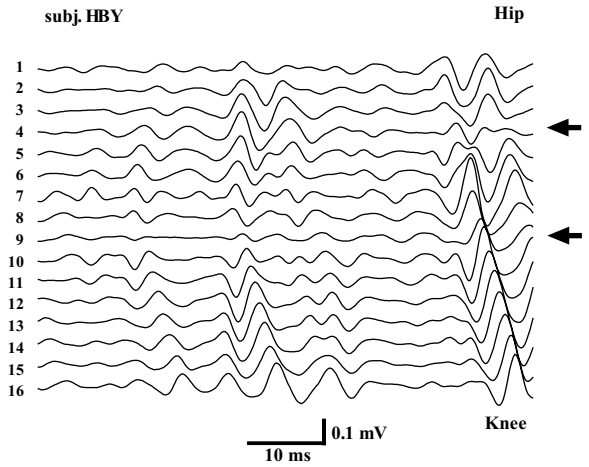

Fig. 11. Waveforms of the surface EMGs detected from the rectus femoris. Arrows indicate the estimated position of the source of the MUAP propagation.

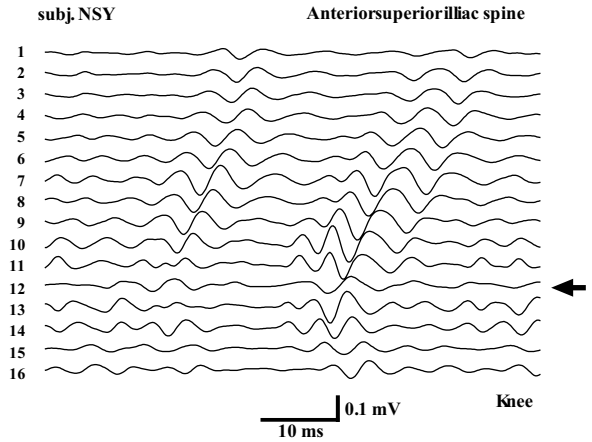

Fig. 12. Waveforms of the surface EMGs detected from the proximal part of the sartorius. Arrow indicates the estimated position of the source of the MUAP propagation.

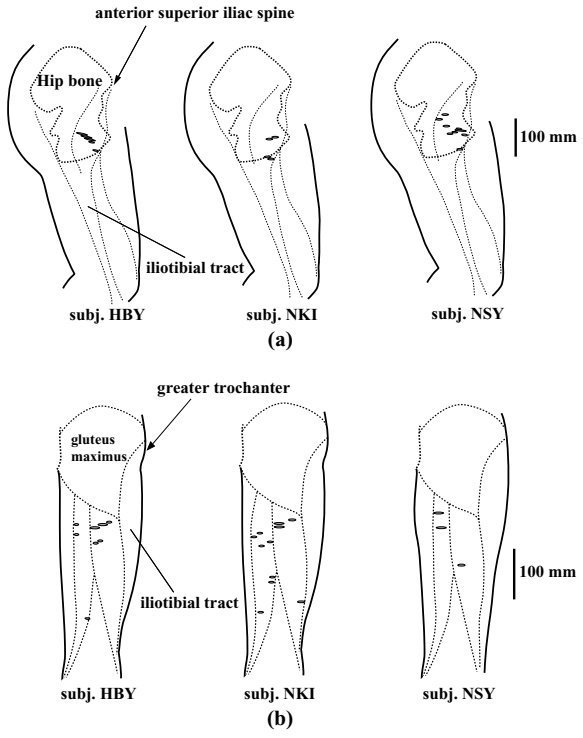

Fig. 13. Distribution of the innervation zones in the tensor fasciae latae (a) and in the semitendinosus and the long head of the biceps femoris (b).

lower leg. These EMGs might be derived from the peroneus longus, while the propagation detected in the distal half of the lower leg might be from the peroneus brevis. The innervation zones of the peroneus longus were distributed in a narrow band around the muscle belly in subject NKI, whereas in subjects HBY and NSY the innervation zones were distributed in a wide area of the muscle belly. The innervation zones located in the distal half, presumably from the peroneus brevis, were identified in subjects NKI and NSY (Figure 15b).

Soleus

The propagation of MUAPs was detected separately in the medial and lateral part of the calf, anterior to the gastrocnemius muscle belly. The muscle fibers of the soleus run diagonally from the posterior inferior portion to the anterior superior portion of the calf. The innervation zones, identified

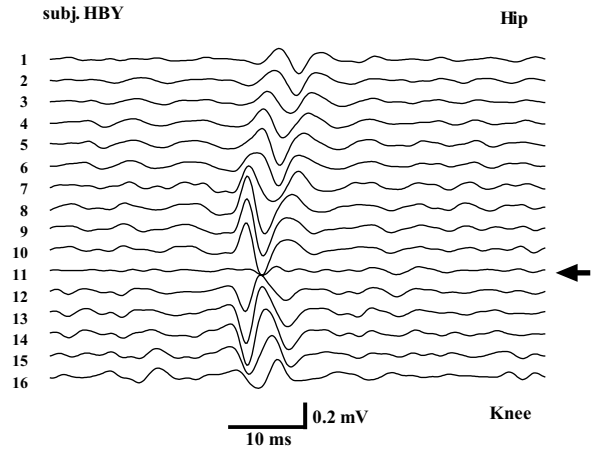

Fig. 14. Waveforms of the surface EMGs detected from the long head of the biceps femoris. Arrow indicates the estimated position of the source of the MUAP propagation.

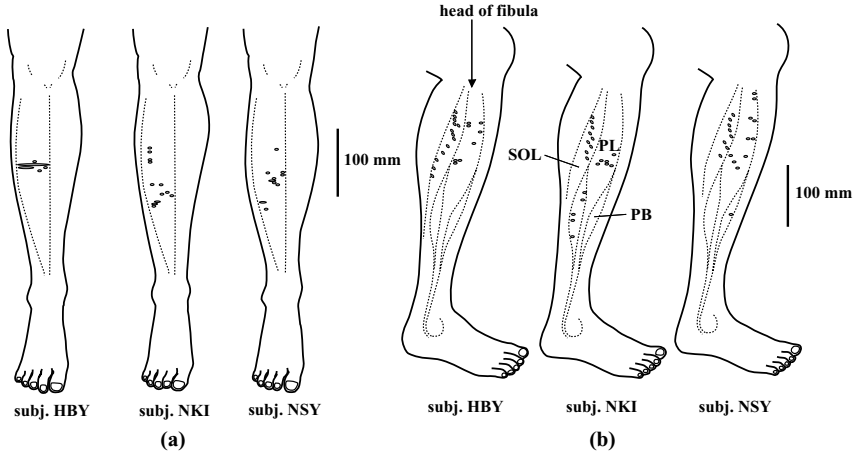

Fig. 15. Distribution of the innervation zones in the tibialis anterior (a) and in the peronei and soleus (b). SOL, PL and PB in (b) indicate soleus, peroneus longus and peroneus brevis, respectively.

longitudinally along the median portion of the muscle fibers, were distributed in a narrow band running diagonally (Figure 15b). They were more abundant in lateral than in medial side (Figure 16a).

Gastrocnemius

The propagation of MUAPs was detected in the circumference of the muscle belly (Figure 17). In the median part of muscle belly, the propagation patterns could not be detected because of the superficial tendinous membrane to which muscle fibers insert. The innervation zones, therefore, were identified in the circumference of the muscle belly in both heads (Figure 16a, b).

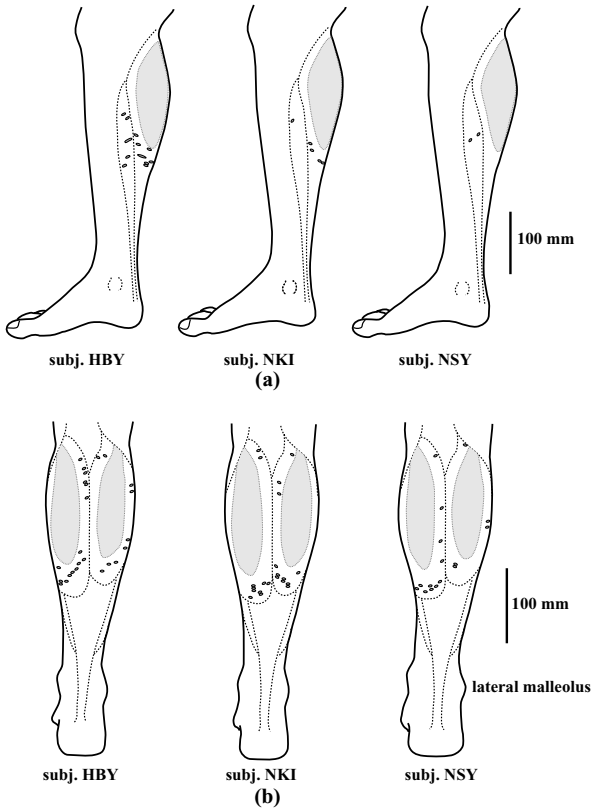

Fig. 16. Distribution of the innervation zones in the soleus and the medial head of the gastrocnemius (a) and both heads of the gastrocnemius (b).

Foot muscles

The propagation of MUAPs could be detected from all the muscles examined. Since the source of the propagation was detected more abundantly from the extensors in the foot than from other muscles, the waveforms of the EMGs were more complex (Figure 19). The innervation zones of the extensor hallucis brevis, extensor digitorum brevis and abductor hallucis were scattered around the muscle belly (Figure 18a, b). In the hypothenar muscles, the innervation zones were distributed in a narrow band around the muscle belly (Figure 18c).

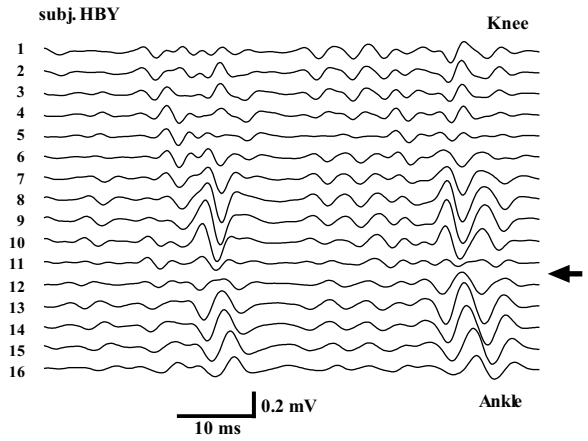

Fig. 17. Waveforms of the surface EMGs detected from the distal part of the medial head of the gastrocnemius. Arrow indicates the estimated position of the source of the MUAP propagation.

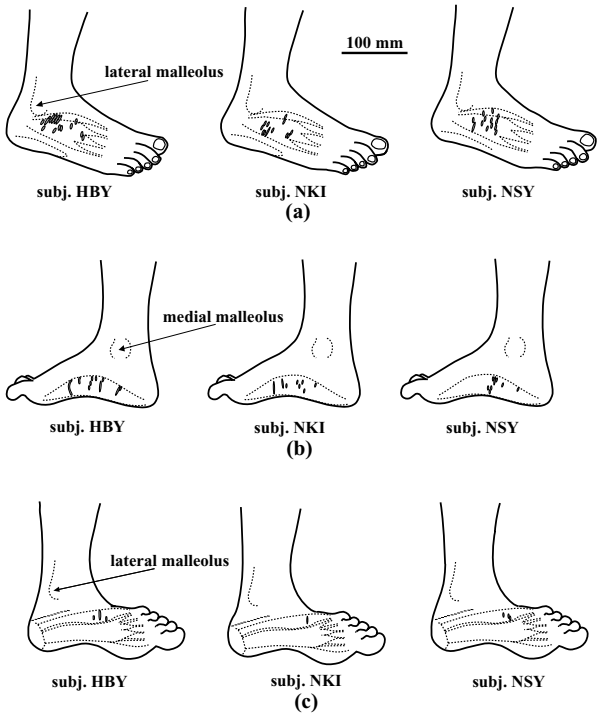

Fig. 18. Distribution of the innervation zones in the extensors in the foot (a), abductor hallucis (b) and hypothenar muscles (c).

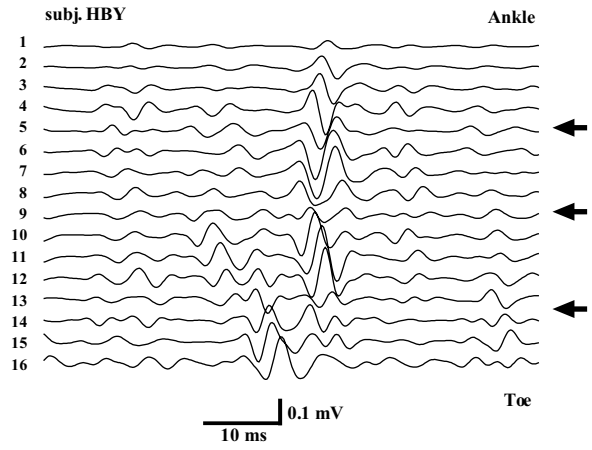

Fig. 19. Waveforms of the surface EMGs detected from the extensors in the foot. Arrows indicate the estimated position of the source of the MUAP propagation.

DISUCUSSION

Detectability of propagating MUAPs and distribution of innervation zones

Christensen (1959), Aquilonius et al. (1984), Hijikata et al. (1992), and Heron and Richmond (1993) studied the distribution of motor endplates in humans and animals by using the cholinesterase staining technique. According to their results, motor endplates were located at the middle length of each muscle fiber, except in the sartorius and gracilis in which they were scattered in the whole muscle belly. Because cholinesterase also exists at the muscle-tendon junction (Aquilonius et al., 1984), the results of the staining may differ from the actual distribution of innervation zones.

As a method to identify the innervation zones non-invasively, Masuda et al. (1983) developed a technique to detect the source of MUAP propagation with multichannel surface EMGs. Masuda and Sadoyama (1987) examined the detectability of propagation of MUAPs in 26 muscles. According to their report, it was relatively easy to detect the propagation of MUAPs in muscles of the upper and lower limb, except the rectus femoris, semitendinosus, gastrocnemius and soleus. Furthermore, Masuda and his colleagues reported in detail the distribution of innervation zones in the biceps brachii, trapezius and lattissimus dorsi (Masuda and Sadoyama, 1991; Shiraishi et al., 1995). According to these authors, such detectability of MUAPs was most likely influenced by the morphology of muscles and structure of the subcutaneous as well as tendinous tissues.

In the present study, the distribution of innervation zones of the upper and lower limb muscles except the biceps brachii was newly clarified. The results of the biceps brachii agreed well with the preceding findings (Masuda and Sadoyama, 1991). Though Masuda and Sadoyama (1987) reported that the innervation zones of the rectus femoris, semitendinosus, gastrocnemius and soleus could not be detected, the distribution of innervation zones of those muscles were preliminarily estimated in the present study. In a majority of muscles examined, the present results basically agreed with the histochemical findings mentioned above that motor endplates were found at the middle length of each muscle fiber (Christensen, 1959; Aquilonius et al.,1984; Hijikata et al.,1992; Heron and Richmond, 1993). Results for the sartorius also agreed with the histochemical findings that motor endplates were scattered in whole muscle belly (Christensen, 1959; Aquilonius et al., 1984; Heron and Richmond, 1993). However, incompatibility with the histochemical findings was observed in muscles

causing difficulties in detecting the propagating MUAPs.

Detectability of the propagating MUAPs depends on matching the direction of muscle fibers to the electrode array. The direction of muscle fibers varies depending on the muscle configuration, which can be fusiform, pinnate, bipinnate or multipinnate. The biceps brachii is a typical fusiform muscle and has muscle fibers running parallel to each other and also parallel to the skin surface. Such an arrangement of this muscle makes the detection of propagating MUAPs easy. Since the intrinsic hand muscles, vastus lateralis and medialis, tensor fasciae latae, tibialis anterior, peronei, soleus and intrinsic foot muscles also have muscle fibers running more or less parallel to each other, the propagating MUAPs of these muscles can be easily detected, too. In these muscles, the innervation zones distributed in a relatively narrow band around the muscle belly.

The innervation zones of the triceps brachii distributed in an inverse U-shaped area surrounding a large tendon attached to the olecranon, because the muscle fibers ran radially from the tendon. The intermediate part of the deltoid is multipinnate and consequently has short muscle fibers running in a complex arrangement. It then becomes difficult to place the electrode array along the muscle fibers, and to detect the propagation of MUAPs. In contrast, the anterior and the posterior parts of this muscle have longer and more parallel muscle fibers (Basmajian and Slonecker 1989), and the detection of propagating MUAPs becomes easier. Resulting, however, from these complex arrangements, the innervation zones of deltoid are scattered in a wide area and the distribution may be shown as an inverse S-shape.

Because superficial muscles in the forearm are thin and have short muscle belly, it is difficult to identify the boundary between the muscles and to place the electrode array along the muscle fibers. Furthermore, the surface EMG recorded from the flexors in the forearm probably included the EMG signals from the flexor digitorum superficialis. These are reasons why the innervation zones of the flexors and the extensors in the forearm scatter in a wide area.

The strap-like sartorius is an exceptional muscle composed of short muscle fibers linked in-series by connective tissues (Christensen, 1959; Heron and Richmond, 1993). Because of this architecture, the streaks of connective tissues are seen in whole muscle surface and the motor endplates distribute all over the muscle (Christensen, 1959; Aquilonius et al., 1984). Our results on the sartorius, that the innervation zones are distributed in the muscle not at the middle length but irregularly on the whole surface, are compatible with the above-mentioned attributes.

In both heads of the gastrocnemius, the innervation zones were distributed in a U-shaped area surrounding the muscle belly because of the muscle fibers running radially from the tendinous membrane located in the center of muscle belly. Though the rectus femoris and hamstrings certainly have bipinnate and pinnate arrangement, respectively, their muscle bellies are large. The reasons are not clear why it was difficult to detect the propagation of MUAPs from these muscles. It is desirable to examine the propagation in subjects who have these muscles with thinner subcutaneous tissues, by adjusting the placement of electrode array relative to the direction of muscle fibers.

Knowledge of the distribution of innervation zones may materialize a variety of applications to be mentioned in the next section. In order to facilitate the applications, simplicity would be preferable in determining the distribution of innervation zones. In the present study, a skillful experimenter distinguished visually between ‘propagating pattern’ and ‘non-propagating pattern’ of surface EMGs. Such a procedure, however, requires an intricate processing of information including the pattern recognition. When we record surface EMG bipolarly with an electrode array from a muscle having muscle fibers running parallel to each other and innervation zones distributing in a narrow band, the amplitude of the EMG picked up with the contacts over the innervation zones becomes diminutive (Masuda et al., 1983; Saitou et al., 1996; Rainoldi et al., 2000). An algorithm incorporating this phenomenon may be useful for estimating the distribution of innervation zones, but only in those muscles having a simple structure, such as the biceps brachii (Masuda and Sadoyama, 1989). It may be difficult in muscles having complicate structure such as the deltoid to automatically identify the innervation zones from surface EMGs. Furthermore, in the examination of such muscles, we could

not place the electrode array exactly along its muscle fibers. Nevertheless, the propagation of MUAPs could be detected if the mal-alignment between the electrode array and muscle fibers was less than about 15 degrees (Sadoyama et al, 1985). Therefore, the methods used in the present study are considered to have robustness and reliability for estimates.

Hägg (1993) has reported that surface EMG measurements become more difficult in female subjects whose fat tissue is more abundant and muscles are smaller than in males. Therefore, the estimation of distribution of innervation zones also may be more difficult in female subjects.

Applications in surface EMG recordings and clinical treatments

As mentioned above, the amplitude of the EMG signals picked up from the locations over the innervation zone becomes diminutive. Roy et al. (1986) have shown that the estimates of the power spectrum and MFCV vary depending on the electrode location with respect to the innervation zone. In dynamic contractions that cause shortening and lengthening of a muscle, the position of the electrodes relative to the underlying muscle tissue may change with time, and consequently affects the EMG amplitude and waveforms (Saitou et al., 1991). In surface EMG recordings, therefore, it is to be desired to avoid the effects of the innervation zone as far as possible. Saitou et al. (1996) have shown that these effects can be arrested by locating the electrodes more than 10 mm apart from the innervation zone.

The present results can be effectively used in recording surface EMGs from limb muscles, especially for amplitude analysis, spectral analysis and MFCV measurements. However, because the location of the innervation zone was different between muscles and also between individuals, it would be difficult to define the typical pattern of its distribution for some muscles in the present results. For muscles in which the innervation zones distributed in a narrow band around muscle belly, such as the biceps brachii, intrinsic hand muscles, tensor fasciae latae, vastus lateralis and medialis, tibialis anterior, and hypothenar muscles in the foot, it would be possible to define the average patterns of distribution by collecting data from a reasonable number of subjects. This would be also possible for muscles in which the innervation zones distributed in particular shapes, such as the triceps brachii and gastrocnemius.

By contrast, for muscles in which the innervation zones were widely scattered and the distribution patterns were different between individuals, such as the deltoid, flexors and extensors in the forearm, rectus femoris, sartorius, hamstrings, peronei, and intrinsic foot extensors, we would have to explore the location of innervation zones before each recording. In addition, it would be beneficial to use miniature electrodes in recording from small muscles.

The present results are important not only for surface EMG recordings but also for clinical diagnosis or treatment of neuromuscular diseases. Knowledge about the position of innervation zones is crucial for the diagnoses of myasthenic syndrome or myasthenia gravis, which include biopsy of the innervation zones called “motor point biopsy” (Ho et al., 1997; Pestronk et al., 1985; Slater et al., 1992). Innervation zones are clinically estimated from motor points detected by electrical stimulation (Roy et al., 1986). Motor points, however, indicate the sites over the skin where the muscle nerve is most sensitive to stimulation. Though most of the motor points are equivalent with the location of innervation zones, cases exist where the both are different from each other. Learning in advance the distribution of innervation zones may be useful in the biopsy. The previous knowledge will be also beneficial in executing efficiently the functional electrical stimulation (FES) and therapeutic electrical stimulation (TES) administered to patients with motor nerve paralysis, in which the motor points are stimulated electrically.

Another possible application is the botulinum toxin injection treatment (Borodic et al., 1991). Botulinum toxin injection is used for treatment of movement disorders with spasticity by blocking release of acetylcholine from presynaptic vesicles at motor endplates. In this case, if the position of innervation zones is known, the treatment will become more effective.

Shiraishi et al. (1995) detected peripheral nerve reinnervation of the trapezius in a subject who

had been subjected to surgical operation, judging from unusual configuration of the innervation zones estimated through multi-channel surface EMGs. If the normal range of the position and the distribution of innervation zones of a muscle can be reasonably determined, abnormal configuration of innervation zones caused, for example, by denervation and reinnervation, may be detected and used for the diagnosis of nerve regeneration.

REFERENCES

Aquilonius, SM, Askmark, H, Gillberg, PG, Nandedkar, S, Olsson, Y, and Stålberg, E (1984) Topographical localization of motor endplates in cryosections of whole human muscles. *Muscle Nerve* **7**: 287-293.

Arendt-Nielsen, L and Zwarts, M (1989) Measurement of muscle fiber conduction velocity in humans: techniques and applications. *J. Clin. Neurophysiol.* **6**: 173-190.

Basmajian, JV and De Luca, CJ (1985) Muscles Alive (5th ed.). Williams & Wilkins, Baltimore.

Basmajian, JV and Slonecker, CE (1989) Grant's Method of Anatomy: A Clinical Problem-Solving Approach (11th ed.). Williams & Wilkins, Baltimore.

Borodic, GE, Cozzolino, D, Ferrante, R, Wiegner, AW, and Young, RR (1991) Innervation zone of orbicularis oculi muscle and implications for botulinum A toxin therapy. *Ophthal. Plast. Reconstr. Surg.* **7**: 54-60.

Christensen, E (1959) Topography of terminal motor innervation in striated muscles from stillborn infants. *Am. J. Phys. Med.* **38**: 65-78.

De Luca, CJ (1984) Myoelectrical manifestations of localized muscular fatigue in humans. *CRC Crit. Rev. Biomed. Eng.* **11**: 251-279.

Hägg, GM (1993) Action potential velocity measurements in the upper trapezius muscle. *J. Electromyogr. Kinesiol.* **3**: 231-235.

Heron, MI and Richmond, FJ (1993) In-series fiber architecture in long human muscles. *J. Morphol.* **216**: 35-45.

Hijikata, T, Wakisaka, H, and Yohro, T (1992) Architectural design, fiber-type composition, and innervation of the rat rectus abdominis muscle. *Anat. Rec.* **234**: 500-512.

Ho, TW, Hsieh, ST, Nachamkin, I, Willison, HJ, Sheikh, K, Keihlbauch, J, Flanigan, K, McArthur, JC, Cornblath, DR, McKhann, GM, and Griffin, JW (1997) Motor nerve terminal degeneration provides a potential mechanism for rapid recovery in acute motor axonal neuropathy after Campylobacter infection. *Neurology* **48**: 717-724.

Masuda, T, Miyano, H, and Sadoyama, T (1983) The propagation of motor unit action potential and the location of neuromuscular junction investigated by surface electrode arrays. *Electroenceph. Clin. Neurophysiol.* **55**: 54-600.

Masuda, T and Sadoyama, T (1987) Skeletal muscles from which the propagation of motor unit action potentials is detectable with a surface electrode array. *Electroenceph. Clin. Neurophysiol.* **67**: 421-427.

Masuda, T and Sadoyama, T (1989) Processing of myoelectric signals for estimating the location of innervation zones in the skeletal muscles. *Front. Med. Biol. Eng.* **1**: 299-314.

Masuda, T and Sadoyama, T (1991) Distribution of innervation zones in the human biceps brachii. *J. Electromyogr. Kinesiol.* **1**:107-115.

Pestronk, A, Drachman, DB, and Self, SG (1985) Measurement of junctional acetylcholine receptors in myasthenia gravis: clinical correlates. *Muscle Nerve* **8**: 245-251.

Rainoldi, A, Nazzaro, M, Merletti, R, Farina, D, Caruso, I, and Gaudenti, S (2000) Geometrical factors in surface EMG of the vastus medialis and lateralis muscles. *J. Electromyogr. Kinesiol.* **10**: 327-336.

Roy, SH, De Luca, CJ, and Schneider, J (1986) Effects of electrode location on myoelectric conduction velocity and median frequency estimates. *J. Appl. Physiol.* **61**: 1510-1517.

Sadoyama, T, Masuda, T, and Miyano, H (1985) Optimal conditions for the measurement of muscle fiber conduction velocity using surface electrode arrays. *Med. Biol. Eng. Comput.* **16**: 651-660.

Saitou, K, Okada, M, Sadoyama, T, and Masuda, T (1991) Effect on surface EMG wave forms of electrode location with respect to the neuromuscular junctions: Its significance in EMG-muscle length relation. *In* Electromyographical Kinesiology, ed. by Anderson PA, Hobart DJ, and Danoff JV, Elsevier Science Publishers BV, Amsterdam, pp 27-30.

Saitou, K, Okada, M, Sadoyama, T, and Masuda, T (1996) Slowing of surface EMG caused by an increase in muscle length. *Jap. J. Electroenceph. Electromyogr.* **24**: 317-324. (*in Japanese*)

Shiraishi, M, Masuda, T, Sadoyama, T, and Okada, M (1995) Innervation zones in the back muscles investigated by multichannel surface EMG. *J. Electromyogr. Kinesiol.* **5**: 161-167.

Slater, CR, Lyons, PR, Walls, TJ, Fawcett, PR, and Young, C (1992) Structure and function of neuromuscular junctions in the vastus lateralis of man. A motor point biopsy study of two groups of patients. *Brain* **115**: 451-478.

Zipp, P (1978) Effect of electrode parameters on the bandwidth of the surface e.m.g. power-density spectrum. *Med. Biol. Eng. Comput.* **16**: 537-541.